

# A ditopic tetradentate pyridyl amine ligand containing an anthracene fragment: fluorescence intensity and 'closed' vs. 'open' species formation in the presence of $\text{Cu}^{2+}$ , as a function of pH

Valeria Amendola, Luigi Fabbrizzi,\*† Piersandro Pallavicini, Luisa Parodi and Angelo Perotti

Dipartimento di Chimica Generale, Università di Pavia, v. Taramelli 12 – I27100 Pavia, Italy

The compounds 9,10-bis(2-pyridylmethylaminoethyl)anthracene  $\text{L}^1$  and 9-(2-pyridylmethylaminomethyl)anthracene  $\text{L}^2$ , based on nitrogen donors of the amine and pyridine type, were prepared and their properties examined in aqueous solution (water–1,4-dioxane 1:4 v/v). The protonation constants of both have been determined by means of potentiometric titrations and the obtained species vs. pH distribution diagrams superimposed on the fluorescence intensity vs. pH profiles. This revealed an 'off-on-off' window behaviour: the fluorescence intensity is high only in the pH range in which both free pyridine and protonated amines exist. Moreover, the formation constants of the complex species which form in the presence of 1 or 0.5 (in the case of  $\text{L}^1$  and  $\text{L}^2$ , respectively) equivalent of  $\text{Cu}^{\text{II}}$  have been determined by means of potentiometric titrations. In particular, in the case of the tetradentate ditopic ligand  $\text{L}^1$  the 'closed' two ligand–two metal species  $[\text{Cu}_2\text{L}^1_2]^{4+}$  and  $[\text{Cu}_2\text{L}^1_2(\text{OH})]^{3+}$  form in basic solution, in addition to two ligand–one metal partially protonated 'open' complex species. Moreover, a strong variation of the fluorescence intensity of the anthracene fragment signals the formation of the 'closed' species with respect to the 'open' ones, while a more subtle variation of the fluorescence intensity also allows one to distinguish between  $[\text{Cu}_2\text{L}^1_2]^{4+}$  and  $[\text{Cu}_2\text{L}^1_2(\text{OH})]^{3+}$ .

The self-assembly of ligands and metals is a subject of intense study. In particular, transition-metal cations, having strong preferences towards certain co-ordination numbers and geometries, may direct the assembly of polydentate polytopic ligands into fascinating supramolecular architectures, including helices,<sup>1</sup> catenates,<sup>2</sup> boxes,<sup>3</sup> squares,<sup>4</sup> pseudo-rotaxanes,<sup>5</sup> racks<sup>6</sup> and grids.<sup>7</sup> The donor groups involved are frequently nitrogen atoms and, accordingly, researchers tend to avoid water or aqueous solutions as the working media in view of the several pH-dependent coexisting species and related equilibria, involving ligand(s), metal ion(s), protons and hydroxide anions. However, from another point of view, if such a complicated situation can be described exactly at each pH value (e.g. by knowing the percentage of each species in the examined pH range), it could be possible to switch advantageously from one species to another and, possibly, from one architecture to another, by simply changing the pH.

Moreover, ligands containing amino groups or pyridine and a fluorescent fragment are known to display a rich photo-physical behaviour in aqueous solution, due to the variation in fluorescence intensity as a function of pH: in particular, a ligand of the pyridine type quenches the fluorescence of a fluorophore like anthracene only when protonated,<sup>8</sup> while an amine fragment quenches the fluorescence of the same fluorophore only when not protonated.<sup>9</sup> In addition, if the pH-dependent interaction of such ligands with transition-metal cations is taken into consideration, in most cases what is observed is a quenching of the fluorescence<sup>9</sup> or, rarely (e.g. with  $\text{Zn}^{\text{II}}$ ), the persistence or revival of it.<sup>10</sup> On this basis, several fluorophore polyamino ligand systems have been used as sensors for protons and/or metal cations in aqueous solutions.<sup>8–10</sup>

In this context it appeared to us particularly appealing to synthesize multidentate polytopic ligands based on nitrogen donors (both of the amine and pyridine type), containing a fluorescent fragment and capable of self-assembling into definite architectures upon interaction with transition-metal cations. In aqueous solutions containing ligand–metal systems

of this type several species are expected to form as a function of pH, and the variation of the emission intensity of the fluorophore may contribute in signalling the existence or prevalence of a particular form. In this work, compounds  $\text{L}^1$  and  $\text{L}^2$  have been prepared (Scheme 1) and the percentage of species distribution vs. pH for the ligands themselves and in the presence of 1 equivalent ( $\text{L}^1$ ) or 0.5 equivalent ( $\text{L}^2$ ) of  $\text{Cu}^{\text{II}}$  fully determined in the range pH 2–12, by means of potentiometric titration experiments. The formation of more than one 'closed' (helical or box-like) structure of 2:2 stoichiometry has been found for  $\text{L}^1$ , depending on the pH value. Moreover, the absorption and emission properties of the ligands and of their complexes with  $\text{Cu}^{\text{II}}$  have been studied as a function of pH and the results compared with the determined species distribution, suggesting that, in the case of  $\text{L}^1$ , fluorescence intensity may signal whether a 'closed' or 'open' complex species is present at a chosen pH value.

## Results and Discussion

### (i) Protonation constants

Although not soluble in pure water, compounds  $\text{L}^1$  and  $\text{L}^2$  can be conveniently dissolved in mixtures of water and organic solvents, such as methanol, acetonitrile or 1,4-dioxane. The latter has been chosen due to its high stability towards acidic and basic hydrolysis, even at the limits of the examined pH range (2–12), a requisite that is necessary when equilibrium constant calculations are to be made on the potentiometric titration data. Thus, potentiometric titrations with standard base were carried out in 1,4-dioxane–water (4:1) solutions containing  $\text{L}^1$  or  $\text{L}^2$  plus an excess of acid. From the obtained data, protonation constants for the examined molecules have been calculated through the HYPERQUAD<sup>11</sup> package. The results are summarized in Table 1 and distribution diagrams (% of species vs. pH) have been drawn for both compounds (see Figs. 1 and 2, solid line).

For  $\text{L}^1$  three consecutive protonation steps are observed, that we ascribe to the formation of  $[\text{HL}^1]^+$ ,  $[\text{H}_2\text{L}^1]^{2+}$  and  $[\text{H}_3\text{L}^1]^{3+}$ . It is interesting that the difference between  $\log K_1$  and  $\log K_2$ , the

† E-Mail: fabbrizz@ipv36.unipv.it

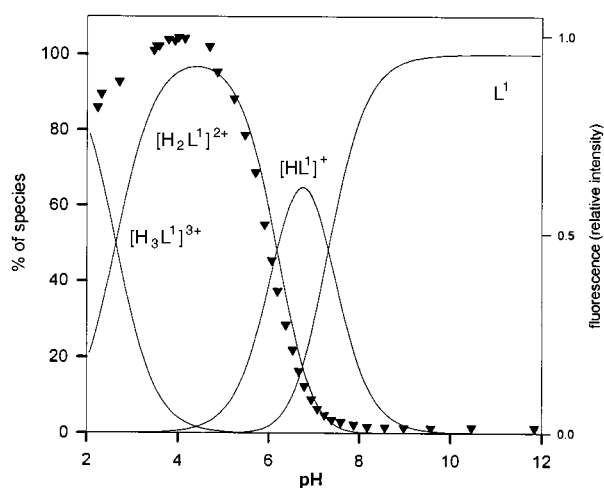
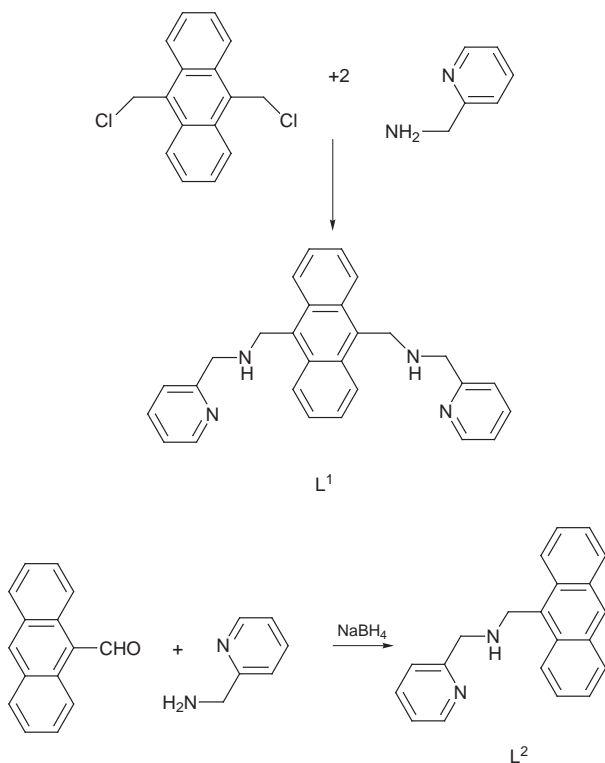


**Fig. 1** Distribution diagram (% of species vs. pH) for compound  $L^1$  in aqueous solution (solid lines, see left vertical axis). The species pertinent to each curve are indicated. The fluorescence of the examined solution is also reported, as relative emission intensity vs. pH (black triangles, see right vertical axis)

two protonation constants involving the secondary amino groups, is quite large (1.13 log units) and overrides the expected statistical advantage for the first protonation step. This is probably due to the formation of an intramolecular hydrogen bridge in the  $[HL^1]^+$  species, between the protonated amino group and the pyridine nitrogen atom belonging to the other half of the molecule, which could make the protonation of the second amino group more difficult. Furthermore, while the third protonation (taking place on one of the pyridine nitrogen atoms) has been determined, data refinement discarded the hypothesis of a fourth protonation process taking place significantly in the examined pH range. This indicates that this protonation, which should involve the last free pyridine nitrogen atom, has such a low formation constant ( $<2$  log units) that  $[H_4L^1]^{4+}$  does not exist in a significant amount in the pH range 2–12.

In the case of compound  $L^2$  two consecutive protonation

**Table 1** Stepwise protonation constants at 25 °C

|            | Equilibrium  | $L^1$             | $L^2$             |
|------------|--|-------------------|-------------------|
| $\log K_1$ | $L + H^+ \rightleftharpoons [LH]^+$                | $7.31 \pm 0.02^a$ | $6.97 \pm 0.02^a$ |
| $\log K_2$ | $[HL]^+ + H^+ \rightleftharpoons [H_2L]^{2+}$      | $6.18 \pm 0.02^a$ | $2.42 \pm 0.02^b$ |
| $\log K_3$ | $[H_2L]^{2+} + H^+ \rightleftharpoons [H_3L]^{3+}$ | $2.64 \pm 0.02^b$ |                   |

<sup>a</sup> Protonation taking place on the amine nitrogen groups. <sup>b</sup> Protonation taking place on the pyridine nitrogen atom.

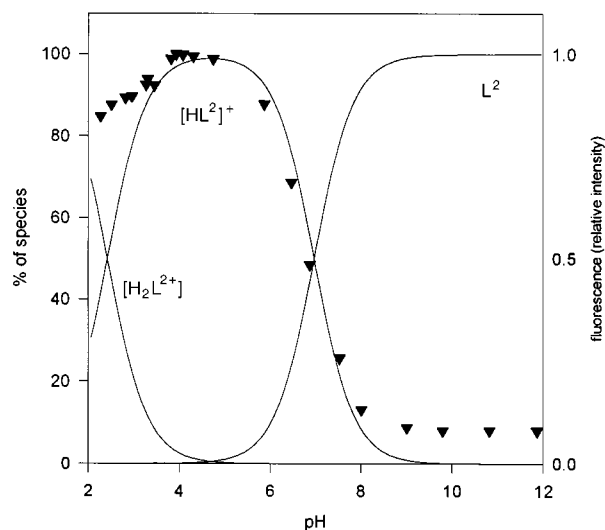


**Fig. 2** Distribution diagram for compound  $L^2$ . Details as in Fig. 1

steps are observed in this pH range, with formation constant values ( $\log K_1$  and  $\log K_2$ , see Table 1) which, as expected, are not much different from those found for analogous processes of the tetradentate  $L^1$  (*i.e.* protonation steps 1 and 3).

### (ii) Complexation with $Cu^{II}$

Compound  $L^1$  is a two-site tetradentate ligand, formed by two bidentate chelating halves of the 2-(aminomethyl)pyridine type, separated by the bulky and rigid spacer anthracene. According to its geometry,  $L^1$  is expected to form with transition-metal cations closed structures of 2:2 (*i.e.* two ligand two metal) stoichiometry, in which each metal cation is co-ordinated by a bidentate site belonging to different  $L^1$  molecules and for which box-like (Fig. 3, form a) or helical (Fig. 3, form b) architectures may be hypothesized.

Fig. 3 schematizes the case in which the metal centre is a copper(II) cation: each copper is co-ordinated by two bidentate 2-(aminomethyl)pyridine units, but is expected to be five-co-ordinated, with a trigonal bipyramidal arrangement, with an additional ligand completing the co-ordination sphere. This hypothesis is supported both by the fact that trigonal bipyramidal geometry is found for comparable  $Cu^{II}$ -ligand systems<sup>12a</sup> and by the spectra displayed by the  $L^1$ - $Cu^{II}$  species, which are consistent (see following discussion for details) with the spectra displayed by authentic trigonal bipyramidal copper(II) centres.<sup>12a,b</sup> As the complexation properties of this system have been examined in aqueous mixtures (and in the absence of any additional co-ordinating species) the fifth co-ordination position must be occupied either by a water molecule or an hydroxide anion, depending on the pH of the solution. Moreover, the formation of closed two metal–two ligand species is expected to take place only under basic or moderately acidic conditions, while under more acidic solutions, also the formation of two ligand–one metal species may be possible (with protons bound to the non-complexed halves of ligands  $L^1$ ), on the basis of what has been reported for several ditopic polyamine ligands, in the presence of  $Cu^{II}$  or other transition-metal cations.<sup>13</sup>

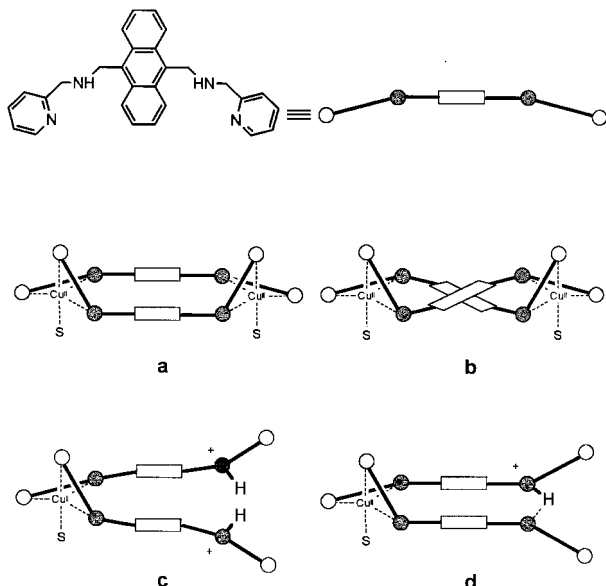


**Fig. 3** Sketches of the hypothesized architectures for the closed  $[\text{Cu}_2\text{L}_2]^{4+}$  species (a, box; b, helix); S represents a molecule of solvent (e.g. water). Sketches c and d describe the monometallic species  $[\text{Cu}(\text{HL})_2]^{4+}$  and  $[\text{CuL}(\text{HL})]^{3+}$ , respectively

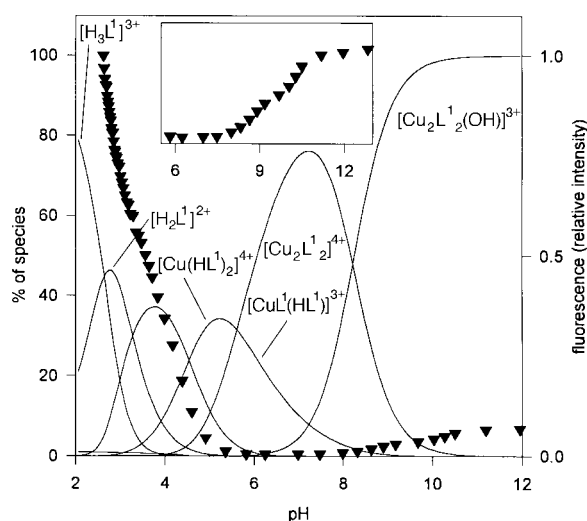


**Fig. 4** Distribution diagram (% of species vs. pH) for the system  $\text{L}^1:\text{Cu}^{2+}$  (molar ratio 1:1). Details as in Fig. 1. An enlargement of the fluorescence vs. pH profile is also reported as inset, for the range pH 6–13

Potentiometric titration experiments with standard base on a 1,4-dioxane–water (4:1) solution of  $\text{L}^1$ , containing 1 equivalent of  $\text{Cu}(\text{ClO}_4)_2$  and an excess of acid, allowed us to determine<sup>11</sup> the formation constants of the metal-containing species existing in solution (see Table 2). From these data, a distribution diagram (% of species vs. pH) can be drawn, which readily visualizes the situation (see Fig. 4, solid lines). As expected, between pH 3 and 7, in addition to some di- or tri-protonated metal free  $\text{L}^1$  species containing two  $\text{L}^1$  molecules, one copper(II) cation and one or two protons exist, although they reach maximum percentages of only 37 (at pH 3.8) and 34% (at pH 5.3) in the cases of  $[\text{Cu}(\text{HL}^1)_2]^{4+}$  and  $[\text{CuL}^1(\text{HL}^1)]^{3+}$ , respectively. It is reasonable to think that in  $[\text{Cu}(\text{HL}^1)_2]^{4+}$  two bidentate sites of two different ligands  $\text{L}^1$  are bound to the  $\text{Cu}^{\text{II}}$ , while the two protons reside on each secondary amino group of the non-co-ordinated halves of the two ligands (as schematized in Fig. 3, e). Moreover, UV/VIS spectra recorded at pH values in which  $[\text{Cu}(\text{HL}^1)_2]^{4+}$  and  $[\text{CuL}^1(\text{HL}^1)]^{3+}$  reach the maximum % value (38 and 35%, respectively) show d–d bands in the

**Table 2** Formation constants at 25 °C for complex species

| Equilibrium  | log K             |
|--|-------------------|
| (a) In the $\text{L}^1\text{--Cu}^{\text{II}}$ (1:1) system  |                   |
| $2\text{L}^1 + \text{Cu}^{2+} + 2\text{H}^+ \rightleftharpoons [\text{Cu}(\text{HL}^1)_2]^{4+}$                                | $27.14 \pm 0.02$  |
| $2\text{L}^1 + \text{Cu}^{2+} + \text{H}^+ \rightleftharpoons [\text{CuL}^1(\text{HL}^1)]^{3+}$                                | $22.60 \pm 0.02$  |
| $2\text{L}^1 + 2\text{Cu}^{2+} \rightleftharpoons [\text{Cu}_2\text{L}^1_2]^{4+}$  | $20.16 \pm 0.02$  |
| $2\text{L}^1 + 2\text{Cu}^{2+} + \text{H}_2\text{O} \rightleftharpoons [\text{Cu}_2\text{L}^1_2(\text{OH})]^{3+} + \text{H}^+$ | $11.95 \pm 0.02$  |
| (b) In the $\text{L}^2\text{--Cu}^{\text{II}}$ (2:1) system  |                   |
| $\text{L}^2 + \text{Cu}^{2+} \rightleftharpoons [\text{CuL}^2]^{2+}$   | $6.90 \pm 0.02$   |
| $2\text{L}^2 + \text{Cu}^{2+} \rightleftharpoons [\text{CuL}^2_2]^{2+}$  | $11.93 \pm 0.02$  |
| $2\text{L}^2 + \text{Cu}^{2+} + \text{H}_2\text{O} \rightleftharpoons [\text{CuL}^2_2(\text{OH})]^{+} + \text{H}^+$            | $3.23 \pm 0.02$   |
| $\text{L}^2 + \text{Cu}^{2+} + 2\text{H}_2\text{O} \rightleftharpoons [\text{CuL}^2(\text{OH})_2] + 2\text{H}^+$               | $-10.16 \pm 0.02$ |

visible region which are typical of a five-co-ordinated trigonal bipyramidal  $\text{Cu}^{\text{II}}$ <sup>12</sup> (a large maximum at 710 nm and a shoulder at 790 nm), indicating that, as expected, a water molecule completes the co-ordination sphere of the metal cation. It is interesting that, from the calculated formation constants, a value of 4.54 log units can be obtained for the protonation constant relative to the process  $[\text{CuL}^1(\text{HL}^1)]^{3+} + \text{H}^+ \rightleftharpoons [\text{Cu}(\text{HL}^1)_2]^{4+}$ . Such a value reflects the increased acidity of the protonated amino groups in  $[\text{Cu}(\text{HL}^1)_2]^{4+}$ , which may be explained on the basis of (i) the large electrostatic advantage for a proton leaving from a tetrapositive molecule, (ii) the repulsion between the two protonated halves of the two  $\text{L}^1$  ligands, which are forced into the same space region by co-ordination of the unprotonated halves to the  $\text{Cu}^{\text{II}}$  and (iii) the formation of a favourable intramolecular ammonium–amine nitrogen bond in  $[\text{CuL}^1(\text{HL}^1)]^{3+}$ , as sketched in Fig. 3, d.

On increasing pH, the  $[\text{Cu}_2\text{L}^1_2]^{4+}$  species forms, reaching 76% in the species vs. pH diagram (Fig. 4) at pH 7.1. Visible spectra recorded at this pH value resemble those found at lower pH {where only  $[\text{Cu}(\text{HL}^1)_2]^{4+}$  and  $[\text{CuL}^1(\text{HL}^1)]^{3+}$  exist} thus indicating a trigonal bipyramidal geometry of the two copper centres, with water molecules completing the co-ordination sphere. The formation constant for  $[\text{Cu}_2\text{L}^1_2]^{4+}$  is 20.16 log units, which, compared with the  $[\text{CuL}^2_2]^{2+}$  formation constant (11.93 log units) reveals some strain in the structure of the  $[\text{Cu}_2\text{L}^1_2]^{4+}$  complex. If the pH is increased over 8 another 2:2 species,  $[\text{Cu}_2\text{L}^1_2(\text{OH})]^{3+}$ , begins to form, reaching 100% at pH 10. The formation of this hydroxide-containing species may easily be followed spectroscopically in the visible region, as the wide maximum found for the d–d band at 710 nm for  $[\text{Cu}_2\text{L}^1_2]^{4+}$  shifts to shorter wavelengths, reaching 615 nm at pH 10, consistent with what is found for deprotonation of the water molecule in other trigonal bipyramidal  $[\text{CuN}_4(\text{H}_2\text{O})]^{2+}$  chromophores.<sup>12</sup>

It must be stressed that on the basis of these data no indication is available on the architecture of the two ‘closed’ species  $[\text{Cu}_2\text{L}^1_2]^{4+}$  and  $[\text{Cu}_2\text{L}^1_2(\text{OH})]^{3+}$ , i.e. as no crystals suitable for X-ray diffraction studies have been obtained it is not possible to discriminate between box-like (Fig. 3, a) or helical (Fig. 3, b) forms. However, molecular modelling ( $\text{MM}^+$ ) calculations through the HYPERCHEM 4.5 package (Hypercube Inc, Canada, 1995) seem to indicate that both for  $[\text{Cu}_2\text{L}^1_2]^{4+}$  and  $[\text{Cu}_2\text{L}^1_2(\text{OH})]^{3+}$  the preferred form is a, featuring the two anthracene fragments almost parallel to each other (average inter-ring distance 3.98 Å) and a distorted bipyramidal geometry at the copper centres.‡

When ligand  $\text{L}^2$  is taken into consideration both species con-

‡ A Referee suggested the hypothesis that, as found for the intramolecular hydrogen bridge in  $[\text{HL}^1]^+$ , species of the  $[\text{CuL}^1]^{2+}$  type may exist in which  $\text{L}^1$  folds on the metal co-ordinated by one half of the ligand and the pyridine of the other half co-ordinates the copper cation in an intramolecular fashion. However, when  $[\text{CuL}^1]^{2+}$  was included in the hypothesized set of species present in solution for the potentiometric data refinement, the data processing discarded it, excluding its presence.

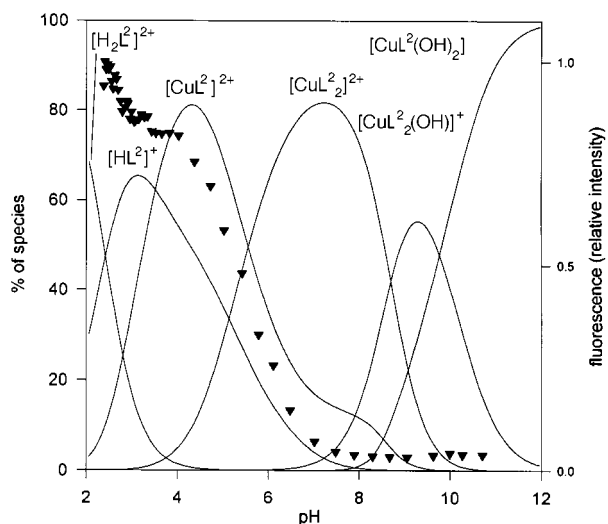


Fig. 5 Distribution diagram (% of species vs. pH) for the system  $L^2:Cu^{2+}$  (molar ratio 1 : 1). Details as in Fig. 1

taining one ligand–one metal and two ligand–one metal are found (see Table 2 and Fig. 5), while the existence of mixed ligand–metal–proton species is ruled out by the structure of  $L^2$ . Species  $[CuL_2]^{2+}$  and  $[CuL_2(OH)]^+$  may be considered as the ‘half’ of the  $[Cu_2L_2]^{4+}$  and  $[Cu_2L_2(OH)]^{3+}$  species found in the case of ligand  $L^1$  and, in this sense, it could be said that the behaviour of  $L^2$  parallels that of  $L^1$ . However, a striking difference is found when high pH values are taken into consideration, as, in the case of  $L^2$ , one ligand is released from  $[CuL_2(OH)]^+$ , to form the  $[CuL^2(OH)_2]$  species (with a water molecule completing the co-ordination sphere, as indicated by UV/VIS spectra in the visible region: at pH >8 the wide maximum found at 710 nm shifts to lower wavelengths, reaching 600 nm at pH 11). The absence of such open forms in the case of ligand  $L^1$ , for which, at high pH values,  $[Cu_2L_2(OH)]^{3+}$  is the preferred form, is reasonably a consequence of the co-operative effect exerted by co-ordination of the two ligands to one copper centre. In the case of  $L^2$ , when  $[CuL_2(OH)]^+$  is disrupted in favour of  $[CuL^2(OH)_2]$ , one ligand is released to the bulk of the solution, but, in the case of  $L^1$ , if one 2-methylaminopyridine unit leaves one of the two copper centres it is still in the presence of a single molecule [the other 2-methylaminopyridine halves are still co-ordinated to the same  $Cu^{II}$ ] and so recombination to give  $[Cu_2L_2(OH)]^{3+}$  is largely favoured.

### (iii) Fluorescence vs. pH

When the fluorescence intensity of compounds  $L^1$  and  $L^2$  is examined as a function of pH in the absence of added metal cations a two-valley one-peak profile is found. The profile can be conveniently superimposed on the distribution diagrams for  $L^1$  and  $L^2$  (see triangles in Figs. 1 and 2, respectively). The maximum in fluorescence intensity is reached at the pH values at which the pyridine fragments are free and the amino groups protonated, *i.e.* when  $[H_2L]^{2+}$  and  $[HL]^{2+}$  reach their maximum percentages. When the solution is made more acidic also the pyridine fragments begin to protonate and, accordingly, the fluorescence intensity falls, due to a quenching process proceeding through an electron-transfer mechanism from the excited anthracene to the pyridinium fragments.<sup>8</sup> On the other hand, when the pH is raised, species containing free secondary amino groups begin to form and, again, the fluorescence intensity falls, due to the electron-transfer quenching process from the free-electron couple on the R–NH–R fragment to the excited anthracene.<sup>9</sup> In this respect, both ligands  $L^1$  and  $L^2$  behave as pH sensors with an ‘off-on-off’ window response,<sup>8</sup> although the low basicity of the pyridine nitrogen in these systems prevents  $[H_3L]^{3+}$  and  $[H_2L]^{2+}$  from forming completely in the pH range

2–12, so that the full fluorescence quenching is not observed in the acidic zone.

The fluorescence of ligands  $L^1$  and  $L^2$  has been examined as a function of pH also in the presence of 1 and 0.5 equivalent of  $Cu^{II}$ , respectively. The resulting  $I_f$  vs. pH profiles are displayed in Figs. 4 and 5 (triangles), superimposed on the % of species vs. pH distribution diagrams. In the case of  $L^1$  the maximum fluorescence intensity is obtained when only protonated species, *i.e.*  $[H_3L]^{3+}$  and  $[H_2L]^{2+}$  exist. On increasing pH, metal-containing species begin to form and, accordingly,  $I_f$  falls, reaching its minimum at pH >5, where only metal-containing species exist. This is due to the ability of transition-metal cations to quench the fluorescence of anthracene through energy-transfer and/or electron-transfer mechanisms.<sup>9</sup> In particular, at the pH values at which  $[Cu_2L_2]^{4+}$  is the prevalent species (pH 7, 80%)  $I_f$  is at its minimum. However, on further increase of pH,  $[Cu_2L_2(OH)]^{3+}$  starts to form and a partial reviving of the fluorescence intensity is observed: although still very low, with respect to that found at pH 2–3,  $I_f$  increases at pH >8, reaching a plateau at pH >10, where  $[Cu_2L_2(OH)]^{3+}$  is at 100% (see Fig. 4, inset). Although on the basis of these experiments no hypothesis can be put forward on the intimate reason for this change, we suggest that the subtle structural and the overall charge changes taking place on transforming  $[Cu_2L_2]^{4+}$  into  $[Cu_2L_2(OH)]^{3+}$  (*i.e.* when a proton leaves one of the co-ordinated water molecules) make the fluorescence quenching process less efficient. In any case, the result is that fluorescence can signal whether  $[Cu_2L_2]^{4+}$  or  $[Cu_2L_2(OH)]^{3+}$  is present in solution.

On observing the  $I_f$  vs. pH curve for  $L^2$  (Fig. 5, triangles) it can be noted that the fluorescence intensity falls on increasing pH, with a profile which almost parallels the % of  $[HL]^{2+}$  vs. pH profile. At pH  $\approx$ 7.5, where only metal-containing species exist,  $I_f$  reaches its minimum. Moreover, it should be noted that on further increase of pH, differently from the case of  $L^1$ , no significant increase in fluorescence intensity is observed when OH-containing species are formed.

## Conclusion

This work has indicated that the use of fluorescent spacers in tetradentate ditopic ligands, based on nitrogen donors of both the pyridine and amine type, leads to interesting molecules. First,  $L^1$  and  $L^2$  act as ‘off-on-off’ pH sensors, in the absence of metal ions. Then, in the presence of  $Cu^{II}$ , closed structures of the two ligand–two metal type form in a restricted pH range, in the case of  $L^1$ . Moreover, the formation of the metal-containing ‘closed’ structures is signalled by a drastic decrease of the fluorescence intensity and, in addition, it has been demonstrated that a further small but significant variation in fluorescence intensity allows one to discriminate between different closed forms. Thus,  $L^1$  may be considered as a prototype of a new class of polydentate polytopic ligand for which the assembly around a metal into a closed architecture is signalled by variations of an easily detectable property such as fluorescence.

## Experimental

### Reagents and materials

2-Aminomethylpyridine and anthracene-9-carbaldehyde from Aldrich were used as such. 9,10-Bis(chloromethyl)anthracene was synthesized according to literature methods.<sup>14</sup>

### Syntheses

**9,10-Bis(2-pyridylmethylaminomethyl)anthracene,  $L^1$ .** 9,10-Bis(chloromethyl)anthracene (0.5 g, 1.82 mmol) was dissolved in toluene (50 cm<sup>3</sup>), a five-fold excess (1.85 g, 17.14 mmol) of 2-aminomethylpyridine added and the mixture heated to reflux for 16 h. The hot solution was then filtered, allowed to return to room temperature and extracted with 0.1 M aqueous  $Na_2CO_3$

(5 × 30 cm<sup>3</sup>), in order to remove the excess of 2-aminomethylpyridine. The organic phase was then dried over Na<sub>2</sub>SO<sub>4</sub>, filtered and the solvent removed on a rotary evaporator, giving a yellow semisolid. On washing with several portions (1 cm<sup>3</sup>) of diethyl ether a yellow powder of L<sup>1</sup> was obtained (Found: C, 80.39; H, 6.22; N, 13.38. C<sub>28</sub>H<sub>26</sub>N<sub>4</sub> requires C, 80.44; H, 6.23; N, 13.31%). NMR (CDCl<sub>3</sub>): δ 4.1 (s, 4 H) and 4.7 (s, 4 H) [NHCH<sub>2</sub>(anthracene) + NHCH<sub>2</sub>(pyridine)], 7.12 (dd, 2 H, H<sup>5</sup> of py), 7.32 (d, 2 H, H<sup>3</sup> of py), 7.45 (dt, 4 H, H<sup>2,3,6,7</sup> of anthracene), 7.61 (dt, 2 H, H<sup>4</sup> of py), 8.3 (dt, 4 H, H<sup>1,4,5,8</sup> of anthracene) and 8.5 (d, 2 H, H<sup>6</sup> of py).

**9-(2-Pyridylmethylaminomethyl)anthracene, L<sup>2</sup>.** Anthracene-9-carbaldehyde (1 g, 4.85 mmol) was dissolved in CH<sub>2</sub>Cl<sub>2</sub> (50 cm<sup>3</sup>) and 2-aminomethylpyridine (0.52 g, 4.85 mmol) dissolved in CH<sub>2</sub>Cl<sub>2</sub> (10 cm<sup>3</sup>) was added dropwise, under a nitrogen atmosphere. The yellow solution obtained was stirred at room temperature for 24 h, giving an orange mixture. After treatment with Na<sub>2</sub>SO<sub>4</sub> it was filtered and evaporated to dryness on a rotary evaporator, to give an orange-brown oily substance, which was then dissolved in CH<sub>3</sub>OH (50 cm<sup>3</sup>) and treated with NaBH<sub>4</sub> (1.5 g) (added carefully and in portions, in order to avoid foaming). The reaction mixture was kept at reflux for 6 h, then the solvent was removed on a rotary evaporator, water (30 cm<sup>3</sup>) added and the suspension obtained extracted with CH<sub>2</sub>Cl<sub>2</sub> (4 × 25 cm<sup>3</sup>). The organic layers were dried over Na<sub>2</sub>SO<sub>4</sub> and the solvent evaporated to give a yellow oil. By dissolving it in the minimum volume of ethanol and treating with an excess of concentrated (37%) hydrochloric acid, the ammonium salt of L<sup>2</sup> was obtained as a yellowish powder. Furthermore, unprotonated L<sup>2</sup> may be prepared (as an oil) by dissolving the ammonium salt in the minimum volume of aqueous 1 M NaOH, extracting with CH<sub>2</sub>Cl<sub>2</sub>, drying over Na<sub>2</sub>SO<sub>4</sub> and removing the solvent on a rotary evaporator (Found: C, 64.90; H, 5.60; N, 7.26. C<sub>21</sub>H<sub>18</sub>N<sub>2</sub>·2HCl·H<sub>2</sub>O requires C, 64.82; H, 5.65; N, 7.20%). NMR (CDCl<sub>3</sub>, free L<sup>2</sup>): δ 4.47 (s, 2 H) and 4.70 (s, 2 H) [NHCH<sub>2</sub>(anthracene) + NHCH<sub>2</sub>(pyridine)], 7.35 (d, 1 H, H<sup>3</sup> of py), 7.55 (m, 5 H, H<sup>2,3,6,7</sup> of anthracene + H<sup>5</sup> of py), 7.87 (dd, 4 H, H<sup>1,4,5,8</sup> of anthracene), 7.94 (dd, 1H, H<sup>4</sup> of py), 8.3 (s, 1H, H<sup>10</sup> of anthracene) and 8.5 (d, 1 H, H<sup>6</sup> of py).

#### Physical measurements and titration experiments

The NMR spectra were recorded on a Bruker AMX 400 instrument, UV/VIS spectra on a Hewlett-Packard 8452 diode-array spectrophotometer. Emission spectra were recorded with a Perkin-Elmer LS-50 luminescence spectrometer (excitation wavelength 378 nm, maximum emission intensity at 424 nm) and were all uncorrected for instrumental response. Spectrofluorimetric titrations were performed in 1,4-dioxane–water (4:1 v/v) solutions (30 cm<sup>3</sup>, 10<sup>-4</sup> M, made 0.1 M in tetrabutylammonium perchlorate); standard HClO<sub>4</sub>, NaOH and Cu(ClO<sub>4</sub>)<sub>2</sub> solutions were used. Potentiometric titrations were performed in 1,4-dioxane–water (4:1 v/v) solutions (50 cm<sup>3</sup>, made 0.1 M in tetrabutylammonium perchlorate) containing L (5 × 10<sup>-4</sup> M), Cu(ClO<sub>4</sub>)<sub>2</sub> (1:1 and 1:0.5 with respect to L, in the case of L<sup>1</sup> and L<sup>2</sup>) and an excess of standard perchloric acid, by addition of standard aqueous NaOH, under a nitrogen atmosphere, in a cell thermostatted at 25 °C. In each titration 50–70 points were recorded. The pH scale was calibrated prior to each experiment with the Gran method<sup>15</sup> (SSCE was used as the reference electrode) by addition of measured quantities of standard aqueous HClO<sub>4</sub> and NaOH to a 1,4-dioxane–water solution (4:1 v/v, made 0.1 M in tetrabutylammonium perchlorate) in the 10<sup>-3</sup> < [H<sup>+</sup>] < 10<sup>-12</sup> range, in which a linear (Nernstian) response was obtained. For low -log[H<sup>+</sup>] values a calibration curve was determined, which takes into account deviations in the emf vs. -log[H<sup>+</sup>] curves from the linear Nernstian behaviour. On this basis, the measured emf in potentiometric titrations could be corrected for the junction potential.

Refinement of the potentiometric data was made through

the HYPERQUAD package<sup>11</sup> which minimizes a least-squares function.<sup>16</sup> A pK<sub>w</sub> of 13.95 was used in the calculations. Attempts to change this value (and, in particular, to increase it, in agreement with that for water–1,4-dioxane mixtures richer in the organic component<sup>17</sup>) gave worse results in the fitting between calculated and obtained emf data. The fit between calculated and experimental emf data was evaluated through σ and χ<sup>2</sup> parameters,<sup>18</sup> which, in each treatment, were found to be 1 ± 0.3 and <11%, respectively.

#### Acknowledgements

This work was supported by the European Union (contract HCM 94-0492). Thanks are due to Dr. Francesca Benevelli (Centro Grandi Strumenti, Università di Pavia) for the NMR measurements.

#### References

- J.-M. Lehn, in *Supramolecular Chemistry*, VCH, Weinheim, 1995, pp. 146–154.
- C. O. Dietrich-Buchecker, J. Guilham, A. K. Khemiss, J. P. Kintzinger, C. Pascard and J. P. Sauvage, *Angew. Chem., Int. Ed. Engl.*, 1987, **28**, 661.
- B. Linton and A. D. Hamilton, *Chem. Rev.*, 1997, **97**, 1669; A. W. Maverick, S. C. Buckingham, Q. Yao, J. R. Bradbury and G. G. Stanley, *J. Am. Chem. Soc.*, 1986, **108**, 7430; M. Fujita, S. Nagao and K. Ogura, *J. Am. Chem. Soc.*, 1995, **117**, 1649; R. W. Saalfrank, B. Horner, D. Stalke and J. Salbeck, *Angew. Chem., Int. Ed. Engl.*, 1993, **32**, 1179.
- M. Fujita, J. Yazaki and K. Ogura, *J. Am. Chem. Soc.*, 1990, **112**, 5645; C. M. Drain and J.-M. Lehn, *J. Chem. Soc., Chem. Commun.*, 1994, 2113; C. A. Hunter and L. D. Sarson, *Angew. Chem., Int. Ed. Engl.*, 1994, **33**, 2313.
- J.-C. Chambron, C. O. Dietrich-Buchecker, J.-F. Nierengarten and J.-P. Sauvage, *J. Chem. Soc., Chem. Commun.*, 1993, 801.
- G. S. Hanan, C. R. Arana, J.-M. Lehn, G. Baum and D. Fenske, *Chem. Eur. J.*, 1996, **2**, 1292; G. S. Hanan, C. R. Arana, J.-M. Lehn and D. Fenske, *Angew. Chem., Int. Ed. Engl.*, 1995, **34**, 1122.
- G. S. Hanan, D. Volkmer, U. S. Schubert, J.-M. Lehn, G. Baum and D. Fenske, *Angew. Chem., Int. Ed. Engl.*, 1997, **36**, 1842.
- A. P. de Silva, H. Q. N. Gunaratne and C. P. McCoy, *Chem. Commun.*, 1996, 2399.
- A. P. de Silva, H. Q. N. Gunaratne, T. Gunnlaugsson, A. J. M. Huxley, C. P. McCoy, J. T. Rademacher and T. E. Rice, *Chem. Rev.*, 1997, **97**, 1515; L. Fabbri, G. Francesc, M. Licchelli, P. Pallavicini, A. Perotti, A. Poggi, D. Sacchi and A. Taglietti, in *Chemosensors of Ion and Molecule Recognition*, NATO ASI series, eds. J. P. Desvergne and A. W. Czarnik, Kluwer, Dordrecht, 1997; L. Fabbri, M. Licchelli, P. Pallavicini, D. Sacchi and A. Taglietti, *Analyst (London)*, 1996, **121**, 1763; L. Fabbri, M. Licchelli, P. Pallavicini, A. Perotti, A. Taglietti and D. Sacchi, *Chem. Eur. J.*, 1996, **2**, 75.
- E. U. Akkaya, M. E. Huston and A. W. Czarnik, *J. Am. Chem. Soc.*, 1990, **112**, 1967; L. Fabbri, M. Licchelli, P. Pallavicini and A. Taglietti, *Inorg. Chem.*, 1996, **35**, 1733.
- A. Sabatini, A. Vacca and P. Gans, *Coord. Chem. Rev.*, 1992, **120**, 389.
- (a) G. De Santis, L. Fabbri, D. Iacopino, P. Pallavicini, A. Perotti and A. Poggi, *Inorg. Chem.*, 1997, **36**, 827 and refs. therein; (b) L. Fabbri, P. Pallavicini, L. Parodi and A. Taglietti, *J. Chem. Soc., Chem. Commun.*, 1995, 2439.
- A. Bencini, A. Bianchi, P. Paoletti and E. Garcia-España, in *Transition Metals in Supramolecular Chemistry*, NATO ASI series, eds. L. Fabbri and A. Poggi, Kluwer, Dordrecht, 1994; R. J. Motekaitis, A. E. Martell, J.-M. Lehn and E. Watanabe, *Inorg. Chem.*, 1982, **21**, 4253.
- M. W. Miller, R. W. Amidon and P. O. Tawney, *J. Am. Chem. Soc.*, 1955, **77**, 2845.
- G. Gran, *Analyst (London)*, 1952, **77**, 661.
- A. Sabatini and A. Vacca, *J. Chem. Soc., Dalton Trans.*, 1972, 1693; A. Sabatini, A. Vacca and P. Gans, *Talanta*, 1974, **21**, 53; P. Gans, A. Sabatini and A. Vacca, *Inorg. Chim. Acta*, 1976, **18**, 239; *J. Chem. Soc., Dalton Trans.*, 1985, 1195.
- E. Wolley, *J. Phys. Chem.*, 1970, **74**, 3908.
- P. Gans, *Data Fitting in the Chemical Sciences*, Wiley, Chichester, 1992.

Received 30th January 1998; Paper 8/00821C